PHYSICAL REVIEW B VOLUME 41, NUMBER 5 15 FEBRUARY 1990-I

Electronic-structure study of the (110) inversion domain boundary in SiC

Walter R. L. Lambrecht and Benjamin Segall
Department of Physics, Case Western Reserve University, Cleveland, Ohio 44106

(Received 14 June 1989; revised manuscript received 12 September 1989)

The linear muffin-tin-orbital (LMTO) band-structure method in conjunction with the local-density-functional method is used to study the electronic and total-energy properties of the (110) inversion domain boundary (IDB) in SiC. This type of boundary occurs frequently in compound semiconductors epitaxially grown on a stepped (001) surface of an elemental semiconductor. Fully self-consistent calculations are presented for a ten-layer superlattice model both for the unrelaxed structure and for a simple bond-rotation–bond-length relaxation model. Calculations for larger superlattices (up to 18 layers) are performed using a restricted self-consistency method which is shown to be in good agreement with the full calculation for the small superlattice. These latter calculations allow us to assess the convergence with cell size and prove helpful in the analysis of the energy of formation. As a result of electrostatic repulsion, a high energy of formation is obtained even when structural relaxation is taken into account. Several interface localized bands are obtained and remain present even after bond-length relaxation. They can qualitatively be interpreted in terms of the formation of Si—Si and C—C bonds near the interface. The *p*-like Si—Si bond related features lie above the SiC valence-band maximum in the semiconducting band gap. With relaxation we even find these states to be pushed up into the conduction band, leading to a semimetallic state and the formation of a two-dimensional electron gas near the IDB. The band-bending effects which can result from local pinning of the Fermi level near the IDB would significantly affect the electrical transport.

I. INTRODUCTION

Recently there has been increasing interest in SiC as an electronic material.[1] Important progress has been made toward the goal of growing high-quality cubic (or β-) SiC films on various substrates.[1–6] The first successful application of the chemical vapor deposition (CVD) process to β-SiC growth was achieved by Nishino *et al.*[2] on a Si substrate. Nevertheless, typical SiC films grown on Si show a large amount of defects such as stacking faults, twins, and inversion domain boundaries (IDB), often called antiphase boundaries (APB). An IDB is an interface between two domains of a nonholosymmetric crystal (here the sphalerite structure) which correspond to each other by an exchange of the two atom types which would be related by an inversion symmetry in the corresponding holosymmetric crystal structure (here the diamond structure).[7] IDB's in SiC have been identified by means of convergent-beam electron diffraction by Pirouz *et al.*[8] These authors proposed that their occurrence is related to monatomic steps on the Si(001) substrate. This problem has been recognized before for other compound semiconductors such as GaAs grown epitaxially on Si(001). It was shown that growing on a vicinal surface a few degrees off (001) which favors diatomic steps[9] inhibits the formation of IDB's in both GaAs (Ref. 10) and SiC.[4,11] However, for SiC on Si, the lattice mismatch is much larger ($\sim$20%). The resulting "vertical" misfit at steps leads to interface dislocations as shown elsewhere[12] and the latter are expected to produce a strain energy four times larger for double steps than for single steps.

The frequent occurrence of the IDB's in epitaxially grown SiC and other compound semiconductors on Si(001) substrates, and the fact that these defects are a very special type of domain boundary, makes them objects of considerable interest. The crystal structure near the IDB is probably much less perturbed than near most grain boundaries. Nevertheless, the chemical effect of interchanging atomic species is strong and thus significant perturbation of the local electronic structure (e.g., the possible introduction of localized interface states) is expected. The study of IDB's is thus in some sense complementary to that of grain boundaries where the perturbation is mostly structural. It is also of interest to compare the IDB with bulk antisite defects, which are point rather than planar defects corresponding to interchange of atomic species. The possible occurrence of interface localized states would have important consequences for the electrical transport as they could locally affect the position of the Fermi level with respect to the band edges and thereby induce band bendings. Finally, antiphase boundaries in intermetallic compounds may play an important role in embrittlement and it seems interesting to consider the corresponding behavior associated with IDB's in semiconductor compounds. As we will see, we expect IDB's in semiconductors to be regions of weak adhesion.

In this paper, we present results of electronic-structure calculations of the (110) IDB in cubic SiC. The (110) crystallographic plane was chosen because it is a symmetry plane of the sphalerite structure. Thus one can construct a supercell with two equivalent boundaries and determine the energy of the defect unambiguously. For other crystallographic planes which are not symmetry planes of the crystal only the sum of the energies of formation of two inequivalent boundaries can be determined straightforwardly by means of the supercell technique. Additional calculations would be required to separate the contributions of each boundary. In this connection we note that the supercell is for practical purposes restricted to correspond to stoichiometric SiC. It is possible, of course, to construct a supercell in the [001] direction with, for example, two equivalent C-C interfaces. But in that case there would be extra layers of C and one could not meaningfully subtract the energy of pure SiC in order to obtain the energy of formation. Instead, one should then subtract the energy of SiC plus an appropriate number of C atoms in some thermodynamic reference state such as a graphitic C reservoir. The ambiguity in choosing the reservoir is an undesirable complication. The (110) plane has the additional advantage of being a nonpolar plane which simplifies the interpretation of the electrostatics. The (110) IDB, which involves both C—C and Si—Si bonds, is more representative of a general IDB than a (111) IDB, which would only involve one type of bond. In fact, IDB's are found to meander randomly along different crystallographic planes throughout the film.[8,13] In the interpretation of electron micrographs, this helps to distinguish them from stacking faults, since the latter only occur along (111) planes. The structural models and our calculational method are discussed in Secs. II and III. Total-energy results are presented in Sec. IV and electronic properties are discussed in Sec. V. Section VI summarizes the conclusions of this work.

II. STRUCTURAL MODELS

As already mentioned in the introduction, an IDB in SiC is an interface between two domains in which the Si atoms and C atoms have been interchanged. Any crystallographic plane can, in principle, separate the two domains. In the case of the (110) nonpolar plane, both a C—C and a Si—Si bond occur across the interface. Figure 1 illustrates the ideal unrelaxed structure. In principle the unit cell extends to $\pm\infty$ along the z direction parallel to [110]. In practice the bicrystal is modeled by means of a superlattice with the IDB periodically repeated every n layers. We denote these superlattices as $(\mathrm{SiC})_n/(\mathrm{CSi})_n$ and have used cells with $n=5,7,9$.

It is obvious that the Si—Si and C—C bonds at the interface in the ideal structure where they have the Si—C bond length (1.89 Å) are heavily stressed. Evidence for local bond relaxation can be obtained from electron microscopy observations[13] since the displacements of the domains with respect to each other gives rise to fringes in the electron micrographs. The fringe spacing and the number of fringes varies with the crystallographic plane. For a (111) IDB only one type of bond, Si—Si or C—C, would occur. In that case, the local bond length can be adjusted simply by a uniform translation of one grain with respect to the other normal to the interface plane. For the (110) IDB, on the other hand, a periodic buckling type of relaxation is expected with stretching of the Si—Si and compression of the C—C bonds. This will lead to some distortion of neighboring bond angles. We have not performed a systematic search of the lowest-minimum-energy configuration. Instead, as a first step, we consider a simple relaxation model in which the Si—Si and C—C bonds are restored to the natural sp^3 bond lengths occurring in the diamond structure (2.35 Å for Si and 1.55 Å for C) while maintaining the Si—C bond lengths unchanged. This seems a reasonable assumption because the tetrahedral coordination is maintained in SiC. Also, it is well known from simple valence force field models[14,15] that bond-angle distortions are much less unfavorable than bond-length distortions. The desired configuration can be achieved by rotating the neighboring Si—C bonds as illustrated in Fig. 2. The angle of rotation indicated in Fig. 2 corresponds to $\varphi=7°$ for the Si—Si bond-length restoring rotation and $\varphi'=6°$ for the C—C bond-length restoring rotation. We note that with this configuration the Si—C bondlengths in the interface layers are very nearly unchanged. Of course, the C—C and Si—Si bonds at the interface are not strictly equivalent to the corresponding bonds in the diamond structure because of the perturbing influence of the neighboring Si—C bonds. Nevertheless, this simple model is expected to be sufficiently accurate to obtain some qualitative conclusions on the relaxation effects. Further work to investigate the structural relaxation is presently under way.

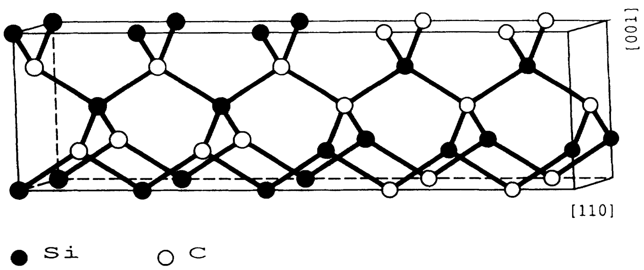

FIG. 1. Unrelaxed structure of the (110) inversion domain boundary in the sphalerite structure.

III. CALCULATION METHOD

We use Andersen's linear muffin-tin-orbital (LMTO) method in the atomic-sphere approximation (ASA) (Ref. 16) for this study. In conjunction with the Hohenberg-Kohn-Sham local-density-functional (LDF) theory,[17] this

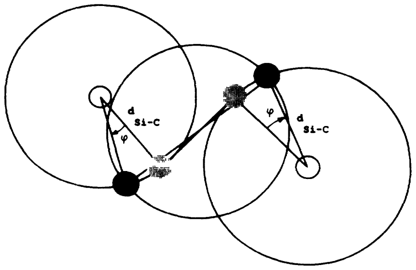

FIG. 2. Bond-rotation bond-length relaxation model. The small open circles denote C atoms, the shaded circles denote Si in the unrelaxed positions, and the solid circles denote Si in the relaxed positions. The relaxed positions are found by rotating the Si—C as indicated until the Si-Si distance of bulk diamond Si is obtained.

method is capable of providing reliable total energies for a wide variety of materials including semiconductors. The ASA is known to have some problems with distorted structures such as frozen phonons and shear distortions. Although this may raise some doubt about the ASA's applicability to the relaxed structural model, we will see that the results obtained are in good agreement with a simple valence force field model. Further, the fact that we are here not dealing with subtle energy differences but rather with strong chemical effects gives us confidence in the applicability of this approximation for this problem. As far as the unrelaxed structure is concerned, ample experience with similar calculations for bulk semiconductors and heterojunctions has shown the adequacy of the ASA.[18–20] In order to minimize systematic errors in the calculation of the energy of formation of the defect, the total energy of perfect SiC was calculated for the same-size supercell as used for the defect and in precisely the same manner. As usual, empty spheres were introduced at the tetrahedral interstitial sites. Fully self-consistent calculations were carried out for the $n=5$ superlattice both in the unrelaxed and relaxed structure.

In order to study the convergence with cell size and for further analysis of the total-energy contributions we have used a "restricted self-consistency" scheme, called the *self-consistent dipole profile* (SCDP) approach, used previously for the study of band offsets,[18,19] dielectric response in semiconductors,[21] and energetics of SiC/AlN interfaces.[20] In the SCDP approach one focuses on the most important degrees of freedom of a layered system: the layer-by-layer variation of the potential. The potential well in each Wigner-Seitz sphere is taken to be the same as in the bulk material except for a constant shift per layer. This constitutes the *frozen-shape* approximation. Because of the variational property of the total energy as a function of the potential, this restricted variational freedom approach is sufficiently accurate for many purposes. The main advantage of this approach, in addition to reducing the computation time by an order of magnitude, is that it leads to a simplified and meaningful expression for the difference in total energy between the system with the defect and the corresponding perfect solid. As we will discuss the various contributions to the total-energy difference in analyzing the results, we give here the necessary details, not presented in our previous discussions of the SCDP approach. The total-energy difference can be shown[22] to consist of three contributions:

$$\Delta E_{\text{tot}} = E^1_{\text{tot}} - E^0_{\text{tot}} \tag{1}$$

$$= \Delta E_{\text{band}} + \Delta E_{\text{Madelung}} + \Delta E^{(2)} \ . \tag{2}$$

The first contribution

$$\Delta E_{\text{band}} = \sum_{\mathbf{R}} \int^{\varepsilon_F^1} N^1_{\mathbf{R}}(\varepsilon)(\varepsilon - \Delta_{\mathbf{R}})\,d\varepsilon - \int^{\varepsilon_F^0} N^0_{\mathbf{R}}(\varepsilon)\,\varepsilon\, d\varepsilon \tag{3}$$

is the change in the sum of one-electron eigenvalues measured on the local scale set by the potential shift $\Delta_{\mathbf{R}}$ on each sphere. It will be called the band-structure term. It reflects changes in the electronic bonding. Here, $N_{\mathbf{R}}(\varepsilon)$ is the local density of states on site $\mathbf{R}$, ε_F is the Fermi energy, and the superscripts and subscripts 1 and 0 refer to the defective and perfect system, respectively. The shifts $\Delta_{\mathbf{R}}$ constitute the variational degrees of freedom of the system. One may use a single average shift per layer or different shifts for each atomic sphere. The former corresponds to the SCDP model used here. In this case, the electrostatics become one-dimensional and the number of parameters is small, which simplifies their self-consistent calculation significantly. Self-consistent determination of the shifts corresponds to an approximate minimization of the ASA total-energy functional with respect to these shifts. The second term

$$\Delta E_{\text{Madelung}} = \tfrac{1}{2} \sum_{\mathbf{R}_1} \sum_{\mathbf{R}'_1 (\neq \mathbf{R}_1)} \frac{q^1_{\mathbf{R}_1} q^1_{\mathbf{R}'_1}}{|\mathbf{R}_1 - \mathbf{R}'_1|} - \tfrac{1}{2} \sum_{\mathbf{R}_0} \sum_{\mathbf{R}'_0 (\neq \mathbf{R}_0)} \frac{q^1_{\mathbf{R}_0} q^1_{\mathbf{R}'_0}}{|\mathbf{R}_0 - \mathbf{R}'_0|} \tag{4}$$

is the change in Madelung energy, i.e., the electrostatic energy of the point charges associated with each sphere in the ASA. The latter is defined as

$$q_{\mathbf{R}} = \int_{s_{\mathbf{R}}} n_{\mathbf{R}}(r)\,d^3r - Z_{\mathbf{R}} = \int^{\varepsilon_F} N_{\mathbf{R}}(\varepsilon)\,d\varepsilon - Z_{\mathbf{R}} \ , \tag{5}$$

where $n_{\mathbf{R}}(r)$ is the spherically averaged electron charge density inside the sphere at site $\mathbf{R}$ and $Z_{\mathbf{R}}$ is the nuclear charge at that site. Throughout this paper, we use atomic units ($e=\hbar=m=1$), in which the unit of energy is the hartree (1 hartree = 27.2116 eV). Note that the Madelung term has to be calculated with the charges of the defect system both for the defect system and for the original perfect system. This may seem somewhat strange but is simply a result of rearranging various Madelung terms in the total-energy-difference expression. In addition, it leads to a simple expression for the Madelung term in the third contribution, shown below. The third contribution

$$\Delta E^{(2)} = \tfrac{1}{2} \sum_{\mathbf{R}} \int \int_{s_{\mathbf{R}}} \Delta n_{\mathbf{R}}(r)\, u(\mathbf{r},\mathbf{r}')\, \Delta n_{\mathbf{R}}(r')\, d^3r\, d^3r' + \tfrac{1}{2} \sum_{\mathbf{R}_0} \sum_{\mathbf{R}'_0 (\neq \mathbf{R}_0)} \frac{\Delta q_{\mathbf{R}_0} \Delta q_{\mathbf{R}'_0}}{|\mathbf{R}_0 - \mathbf{R}'_0|} \tag{6}$$

consists of various second-order terms: intra-atomic and interatomic. They correspond to the change in charge density in each sphere. The interatomic, or Madelung, contributions to these terms is calculated with the changes in each point charge. This second-order Madelung contribution appears as a result of the rearrangement of Madelung terms referred to above. The intra-atomic term is basically the self-energy of the change in charge density inside each sphere and the interaction contains a Hartree and an exchange-correlation part:

$$u(\mathbf{r},\mathbf{r}') = |\mathbf{r}-\mathbf{r}'|^{-1} + \delta(\mathbf{r}-\mathbf{r}')\,\partial\mu_{\text{xc}}[n^0(r)]/\partial n \ . \tag{7}$$

In practice, the latter is small and may be neglected, although it is not especially difficult to evaluate. Moreover, since $\Delta E^{(2)}$ itself is small (it turns out to be only about 10% of ΔE_{tot}), it is justifiable to further simplify it. This can be done by replacing $\Delta n(r)$ inside the sphere by its volume average over the sphere. This leads to the very simple estimate

$$\Delta E^{(2)}_{\mathbf{R}} \approx 3(\Delta q_R)^2/5s_R \tag{8}$$

for the intra-atomic second-order contribution of site **R**. Note that in this approximation, only the changes in total charge per sphere are used. The $\Delta n(r)$ functions are not needed, which means a significant simplification of the computer codes. This additional approximation was used in the calculations reported here.

A very attractive feature of this "frozen-potential" formalism is that it resembles the total-energy-difference expression used in tight-binding calculations.[23,24] In fact, the total-energy difference is basically expressed as a change in the sum of the occupied one-electron eigenvalues plus some repulsive terms. The self-consistency treatment is also similar to a tight-binding treatment where only diagonal terms of the Hamiltonian are adjusted to reflect charge transfer. The above equations are only valid assuming the sphere sizes do not change, i.e., assuming volume conservative changes. The formalism applies both to structural changes (displacing atoms) and chemical changes (interchanging atoms on a given structure). However, the errors made due to the overlap of the spheres in the ASA may become unacceptably large for certain structural changes. The method is thus mostly suited for chemical changes such as alloy energy of formation, superlattice energy of formation, or the present IDB problem, since in these cases the ASA-induced errors largely cancel.

IV. TOTAL-ENERGY RESULTS

We first present some results obtained for pure cubic SiC in order to gauge the accuracy of the LMTO-ASA calculation method for this material. The equilibrium lattice constant was calculated to be 4.31 Å [expt. (Ref. 25) 4.36 Å], the bulk modulus was calculated to be 231 GPa [expt. (Ref. 25) 224 GPa], and the cohesive energy, including zero-point motion correction of 0.105 eV/cell and spin-polarization corrections for the atoms of 0.64 eV/atom for Si and 1.16 eV/atom for C, was calculated to be 7.15 eV/atom [expt. (Ref. 26) 6.34 eV/atom]. The overestimate of the cohesive energy is a well-known failure of the local-density approximation (LDA). Our slight underestimate of the lattice constant is mostly due to the neglect of the so-called combined correction term.[16]

Next, we consider the energy of formation of the IDB calculated by subtracting the total energies of the same-size supercells with and without the IDB. Note that two IDB's occur per supercell. Table I shows the energy of formation of the unrelaxed and relaxed IDB obtained from the fully self-consistent ASA calculation for the $n=5$ supercell. The energy of formation of the unrelaxed IDB for the superlattices $n=5,7,9$ and the various contributions obtained within the SCDP approach are also shown. Excellent agreement is obtained between the more approximate SCDP calculation and the ASA calculation. The SCDP gives a slightly higher value, as expected, because of the limited variational freedom. The SCDP calculations for larger cells show that the results for the $n=5$ cell is converged regarding cell size to within 0.1 eV.

The Madelung contribution may be seen to converge most slowly. The fact that the net layer charges on the central layers of the cell are truly negligible in the 9+9 cell—see Fig. 5 below—suggests that convergence has been reached. However, we emphasize that the Madelung energy here involves the charge distribution per atom, not just the average per layer. To some extent, the rather slow convergence of the Madelung energy in Table I could be due to the fact that only the layer average has been made self-consistent in the SCDP approach.

Table I shows that the electrostatic contribution to this energy is very important. This is easy to understand if one realizes that SiC is actually quite ionic because of the deep-lying C valence orbitals. On the recently proposed tight-binding LMTO polarity scale,[18,27] it has a polarity of 0.473, compared e.g., to 0.404 for GaAs. As this polaricty scale is based on the partial wave components of the wave function within the spheres, the fairly large ionicity of SiC is related to the choice of equal sphere radii for C and Si. Conventionally, a smaller atomic radius is associated with the C atom than with the Si atom and thus less charge is associated with the C atom, which leads to a somewhat lower ionicity. On the well-known Phillips ionicity scale,[28,29] SiC has an ionicity of 0.177 compared to 0.310 for GaAs. The difference in the static (9.72) and dynamic (6.52) dielectric constants,[25] however, also supports a rather large ionicity, in agreement with our polarity scale. Although the value of the ionicity (or polarity) is thus somewhat ambiguous, a certain degree of ionicity of the bonding is clearly present. The arrangement with opposing equal charges at the IDB is energetically very unfavorable. The band-structure contribution,

TABLE I. Interface energy of formation of the (110) inversion domain boundary in SiC in eV/interface–unit-cell–area.

		Unrelaxed				Relaxed
		SCDP			ASA	ASA
n	ΔE_{band}	$\Delta E_{\text{Madelung}}$	$\Delta E^{(2)}$	ΔE_{tot}	ΔE_{tot}	ΔE_{tot}
5	2.142	3.236	0.724	6.10	5.91	3.02
7	2.140	3.200	0.717	6.06		
9	2.140	3.185	0.716	6.04		

however, is also substantial and will be discussed below in connection with the electronic properties. In the unrelaxed model, a small positive over-pressure of 12 GPA was obtained[30] compared to the perfect crystal, indicating that the system is not in equilibrium and has a tendency to expand.

The effects of structural relaxation are considered next. The $n = 5$ superlattice and a fully self-consistent ASA calculation was used for this purpose. The simple Si—C bond rotation and Si—Si, C—C bond-length relaxation model discussed in Sec. II was found to be energetically favorable with respect to the unrelaxed structure by 2.89 eV per interface–unit-cell area (henceforth i.u.c.a). At the same time the change in pressure with respect to the perfect crystal became slightly negative (-3 GPa) indicating that we approached the equilibrium. Although we cannot confirm with certainty that the relaxation model investigated corresponds to the lowest-energy configuration, the sizable reduction in energy indicates that the model is at least a reasonable guess. Further work on the atomic relaxations is in progress.

Our calculation for the relaxation energy is in excellent agreement with a simple estimate based on Keating's valence-force-field model.[14] This is obtained by neglecting the bond-angle distortion contributions to the energy and using the bond-stretching force constants fitted to the elastic constants of Si and C in the diamond structure (48.50 N/m for Si and 129.33 N/m for C).[15] We find that relaxing the Si—Si and C—C bond from the Si—C bond length (1.89 Å) to the diamond Si—Si (2.35 Å) and C—C (1.55 Å) bond lengths reduces the energy by 2.99 $\mathrm{J\,m^{-2}}$ or 2.50 eV/i.u.c.a. Within this model, this is an upper limit of what may be gained by relaxation of the bonds because the latter will cost some bond-bending energy.

For the relaxed geometry we thus obtain 3.02 eV/i.u.c.a. as indicated in Table I. We point out that this energy per unit-cell area corresponds to 3.6 $\mathrm{J\,m^{-2}}$. This is huge compared to the energy of the other frequently occurring planar defect in SiC, the stacking fault. The latter is of the order 10^{-3} $\mathrm{J\,m^{-2}}$.[31,32] It thus may seem surprising that IDB's nevertheless occur frequently. This, however, is a consequence of the growth process on stepped surfaces and the topological nature of this defect, which cannot be eliminated by means of dislocations. As already mentioned, their occurrence can be largely prevented by growing on a vicinal surface of the Si substrate slightly off axis of the (001) plane. The fact that numerous stacking faults remain present in this case while IDB's disappear almost completely is consistent with the much lower energy of the former. However, there are indications that also the occurrence of stacking faults is related to the three-dimensional growth mode.[33]

The high interfacial energy indicates that IDB's are places of significantly weakened adhesion. The IDB interface energy is comparable in magnitude to the surface cleavage energy. Based on a simple bond-breaking argument, which we have previously shown to yield reasonable values,[20] the latter should be about one bond energy or one quarter of the cohesive energy per bulk unit cell. This would amount to 3.5±0.5 eV/surface-unit-cell–area for SiC. Here we do not include the spin-polarization correction or zero-point motion corrections but assume the surface energy to be somewhat lowered by relaxation. The adhesion energy W_a at an IDB is given by

$$W_a = 2\gamma_s - \gamma_i , \tag{9}$$

where γ_s is the surface cleavage energy and γ_i the above-calculated interface energy. The adhesion energy is then found to be of the order of 4.0±0.5 eV/i.u.c.a In other words, the adhesion energy gained when joining two surfaces in the normal way with Si—C bonding (i.e., $2\gamma_s \approx 7$ eV) is reduced to about half its value when joining them at an IDB, which has Si—Si and C—C bonds. The weak adhesion at an IDB does not necessarily mean that the latter would degrade the strength of the material as a whole. To the contrary, the existence of weak interfaces may lead to toughening of a brittle material because the cracks can be stopped at interfaces instead of running through the sample. The weak interfaces can thus prevent failure of the system as a whole.

Finally, we mention that our energy of formation per cell for the IDB is of the same order of magnitude as the average energy of formation of antisite point defects.[34] The latter also involve either Si—Si bonds (for the $\mathrm{Si_C}$ defect) or C—C bonds for the $\mathrm{C_{Si}}$. Nevertheless, the bonding environment is quite different from that near the IDB. It turns out that the $\mathrm{C_{Si}}$ defect has a much lower formation energy (1.1 eV) than the $\mathrm{Si_C}$ defect (7.3 eV).

V. Electronic Properties

In this section we present results for the interface band structure, the charge distribution and potential profile, and related electronic properties.

A. Layer projected densities of states

The layer projected densities of states for the relaxed and unrelaxed superlattices are shown in Fig. 3. These were obtained using the tetrahedron method with 48 **k** points in the irreducible part of the supercell Brillouin zone. To avoid unphysical spikes, the densities of states were broadened with a Gaussian of 0.2-eV width. The vertical lines in these figures indicate the band edges of pure SiC near the two gaps and the Fermi levels. The lower gap occurs between the mainly C 2*s*-like states and the C 2*p* to Si bonding states. The higher gap is the semiconducting gap between the uppermost valence band and the conduction band. The Fermi level for each system corresponds to neutral IDB superlattices.

By comparing the interface layer (layer 1) with a reference calculation for pure SiC, the following interface-induced features can be discerned. For the unrelaxed model the lower band gains intensity in the low-energy region below −11 eV and a peak splits off at the upper end into the lower gap. This peak lies at about −9 eV. The upper part of the valence band, which basically has a lower peak around −7 eV and a higher peak between −3 and 0 eV with a shoulder at −4 eV, has all of its features broadened. Some states tail into the lower band gap and some tail into the upper band gap, in fact, completely filling the latter. The neutral IDB superlattice effectively becomes a semimetal with the Fermi level pinned at the bottom of the conduction band. Upon relaxation the perturbation of the density of states becomes even more pronounced. The states tailing into the upper gap form a separate peak, which is pushed up into the conduction band where it forms a resonance. The Fermi level gets pushed up further, residing in a region of low density of states just above the resonance. Although the interface localized features clearly decrease as one moves towards the central layer, they are not at all negligible on the latter. This indicates that superlattice effects, that is, interactions between the two interfaces per supercell, are significant.

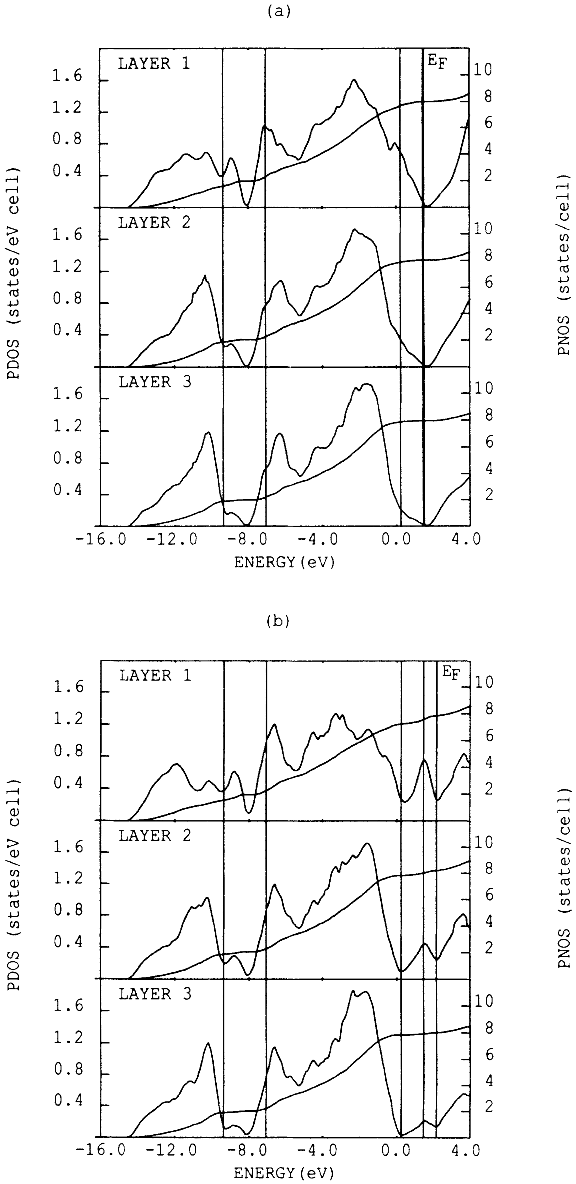

FIG. 3. Layer projected density and number of states functions (PDOS and PNOS) for a 10-layer superlattice. (a) Ideal structure; (b) relaxed model. The vertical lines indicate the edges of the bands of pure SiC and the Fermi energy for a neutral IDB.

B. Dispersion of interface states

Details of the superlattice band structure along the three principal directions are given in Fig. 4. The $\Gamma-X$ line corresponds to the cubic [001] direction and the $\Gamma-Y$ line to the $[1\bar{1}0]$. The $Y-B$ line corresponds to the [110]

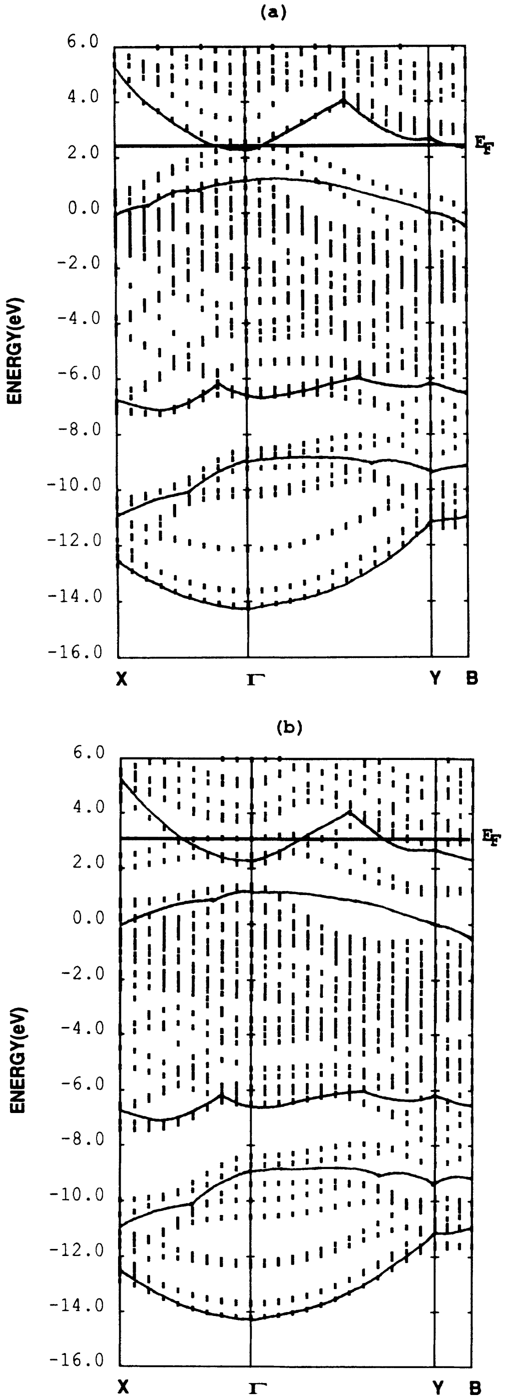

FIG. 4. Supercell band structure along high symmetry lines. (a) Ideal structure; (b) relaxed model. The **k** points are described in the text. The solid lines correspond to the edges of the pure SiC band structure represented in the same superlattice Brillouin zone. The Fermi level indicated corresponds to a neutral IDB supercell.

superlattice direction along which the dispersion is fairly small, as expected. The band edges of the pure SiC band structure when plotted along the same high-symmetry lines are shown by solid lines. Note that the conduction-band minimum at point X_{fcc}, which is equivalent to the point $(\pi/a,\pi/a,0)$, is folded onto the Γ point in any (110) superlattice with an even number of layers.

The following interface features can be seen. Two bands split off from the upper end of the lower valence band and from the bottom of the upper valence band. Also, two bands are pushed out from the upper band into the higher band gap. In the case of the relaxed model, the latter two are pushed into the conduction band. A segment of a band above the valence-band edge (which is nearly twofold degenerate) and two segments slightly below the conduction-band edge are also evident. Since their marginal location in the gap might well result from a superlattice perturbation, we cannot with any degree of certainty identify these states with the interface.

The occurrence of all the main interface features in pairs of two is also a superlattice artifact arising from the interaction between the interface localized states of the two interfaces. The strongly **k**-dependent splitting of these states varies between 0.0 and 1.0 eV. In a very large supercell this splitting should go to zero leading to twofold-degenerate interface bands. We have studied large superlattices up to 18 layers by means of the SCDP approach. For the $5+5$ superlattice, the densities of states obtained by means of this approach were practically indistinguishable from the previous fully self-consistent ASA results. For larger superlattices, results similar to those for the smaller one were obtained. The splitting of the interface bands at a given **k** point was found to decrease with increasing superlattice size. The layer projected densities of states on the fifth layer away from the interface were found to be practically negligible for energies in the gaps of SiC, suggesting bulk behavior. Nevertheless, the splitting was still not negligible, showing that very large supercells would be necessary for an accurate study of the isolated interface states. A Green's-function method,[35] which enables one to study a single interface with truly semi-infinite boundary conditions, would clearly be preferable for this purpose. The practical implementation of this approach is still in development. Inspection of the eigenstates at Γ confirms the interface localization of the aforementioned states. It shows that the states right at the edge of the valence bands show localization and contribute to the peak near 0 eV in Fig. 3(a). The considerable dispersion of the interface bands relates to the broadness of the features in the densities of states.

C. Origin of the interface states

It is instructive to obtain an understanding of the origin of the above-noted modifications in the band structure. This we achieve through the use of a simple bond-orbital model for semiconductors developed by Harrison.[36] In this model sp^3 hybrid orbitals are constructed from atomic orbitals and the most prominent interaction occurs between nearest-neighbor orbitals pointing toward each other. This interaction, called V_2 by Harrison, is taken to be the universal function of distance d between the orbitals $V_2=-3.22/d^2$. Within this model, the interaction corresponding to Si—Si, Si—C, or C—C bonds is the same when the distance between the atoms is the same (i.e., for the unrelaxed model). For the SiC bondlength, $V_2\approx-7$ eV. The energy levels of the hybrids $(\varepsilon_s+3\varepsilon_p)/4$ can be obtained from tabulated atomic energy levels (see Ref. 36), and the level for C is found to be about 4 eV deeper than for Si. A simple calculation then shows that when all bondlengths are taken to be that of SiC the Si—Si bonding state lies about 2 eV higher than the Si—C bond, which in turn lies about 2 eV higher than the C—C bond. The same is true for the corresponding antibonding states. The interactions between neighboring bonds broadens each of these levels into bands, and the tetrahedral crystal field leads to a splitting into s-like and p-like states. Despite the broadening and splitting, the very simple model leads one to expect the Si—Si-bond-related features to be pushed up and the C—C-bond-related features to be pushed down in energy relative to the SiC features. This indeed corresponds to all the changes in the spectra near the interface. The reasoning can be applied separately to the s-like states and to the p-like states, i.e., to the lower and upper bands, respectively. Purely Si or purely C-related features (from the Si—Si and C—C bonds) are, of course, not observed as the fairly strong interaction with the neighboring bonds (Harrison's metallicity effect) admixes other atomic character into the wave function for the bond. Also, some interaction between the C—C antibonding state and the Si—Si bonding state is conceivable, although these bonds are separated by second-nearest-neighbor distances. Relatedly, the atom resolved partial densities of states show essentially the same relative C and Si contributions in the interface features as in the bulk SiC features. The lower band is predominantly C related and the states near the top of the valence band have about equal C and Si contributions.

Upon relaxation of the bondlengths, one expects the Si—Si interaction to decrease and the C—C interaction to increase. This will push the Si—Si-bond-related features further up in energy and the C—C-related features further down in energy. These effects agree with the observed changes in the spectra introduced by the relaxation. In particular, they are in accord with the fact that the upper interface band gets pushed up further into the conduction band.

Because of the opposite effects of the relaxation on C—C and Si—Si bonds, the net contribution to the total-energy difference is not obvious. It turns out that the relaxation increases the band-structure contribution to the energy. On the other hand, it leads to a decrease in the Madelung energy, which is larger than the positive change in the band-structure energy. As noted in Sec. IV, the total energy is lowered by about 3 eV. We wish to reiterate that our relaxation model was only a plausible surmise. While the significant lowering of the total energy lends support to the model, we cannot exclude further reconstructions or relaxations.

D. Discussion of the interface states

An important result of the calculation is that even after relaxation of the bond lengths the interface states are still present. It is interesing to note that Wang *et al.*[34] find that no defect states in the gap occur for bulk antisite defects in SiC. Obviously, the two-dimensional nature and the lower symmetry make the IDB very different from the bulk antisite defects in spite of the fact that both involve Si—Si and/or C—C bonds.

At present there are only limited experimental data available on the IDB. Photoluminescence studies of SiC (Ref. 37) grown epitaxially on Si(001) show broad features, labeled as the *G* bands, which have been ascribed tentatively to extended defects. However, these features occur at about 1.9 eV, whereas transitions between the lowest unoccupied states and the highest occupied states near the neutral IDB are expected at much lower energies according to our present calculation. Allowing for some uncertainty in the position of the highest occupied interface band we expect such transitions to occur in the range 0.0–0.5 eV, i.e., well in the infrared region. Photoluminescence data in this energy range are not available to the best of our knowledge. In ir absorption, these features could overlap with the vibrational transitions but the latter are not expected to be present in the photoluminescence spectra because of the low temperature at which these experiments are carried out.

The most recent photoluminescence experiments[38] indicate that the *G* bands are still present for samples free of IDB's and thus are presumably related to other defects. In fact, these samples still show a considerable amount of stacking faults and dislocations.

We hope that this work may inspire more detailed experimental investigations of IDB induced electronic states. As indicated above, it would be interesting to look for photoluminescence bands in the ir region and also it would be worthwhile to study the photoluminescence as a function of the doping of the sample. As the interface states are occupied and cover almost the entire band gaps, it might also be possible to pick up a signal from them in photoemission studies of samples with a high density of IDB's as compared to IDB free samples. The density of IDB's in the sample could be effectively increased by focusing on a thin region near the interface with Si.

E. Discussion of the semimetallic nature

The semimetallic nature of the IDB supercell deserves some discussion. First of all, we call the system a semimetal rather than a metal, because the metallicity is due to a nearly filled valence band which is slightly overlapping with the mostly empty conduction band. This situation is typical for a semimetal such as, e.g., Sn or HgTe.

As is clear from Sec. V B, the artificial superlattice splitting of the interface band contributes to the degree of semimetallicity of the system. In the unrelaxed model, the center of gravity of the two bands corresponding to a single interface band for an isolated interface occurs below the conduction-band edge and thus a larger superlattice would presumably not be metallic. For the relaxed case, the center of gravity of these bands lies in the conduction band so that the system could remain semimetallic even for larger superlattices. However, the interface state wave function for an isolated IDB could spread out further, thereby reducing the Coulomb repulsion and presumably lowering the interface state. Thus, even in the relaxed case, it is not clear whether or not the semimetallic nature near the interface would be maintained.

If the semimetallic state is found to occur even for a single IDB, it still does not mean that the whole system becomes a semimetal. Rather one should then consider the IDB as a two-dimensional (semi)metallic system. In fact, one can think of the system as a whole as two Schottky barriers back-to-back with the Fermi level locally pinned just above the bottom of the conduction band. In the rest of the semiconductor a band bending would occur as dictated by the constancy of the Fermi level throughout the system and the appropriate position of the Fermi level in the bulk semiconductor far away from the interface. The interface region would then correspond to a two-dimensional electron gas similar to the situation occurring in metal-oxide-semiconductor field-effect transistors (MOSFET's) or in doped quantum-well systems. As is well known, such a system has very intriguing properties such as the quantum Hall effect. It is very interesting that such a two-dimensional electron gas could possibly occur in a single material near a planar defect. Unfortunately, IDB's usually are not confined to a single crystallographic plane and occur usually in samples with a lot of other defects. Experimental verification of this possibility would thus appear to be extremely difficult.

F. Charge distribution and potential profile

Also of considerable interest are the charge distribution and the associated electrostatic potential profile. Figure 5 shows the layer-by-layer average charge distribution and potential near the (110) IDB as obtained form

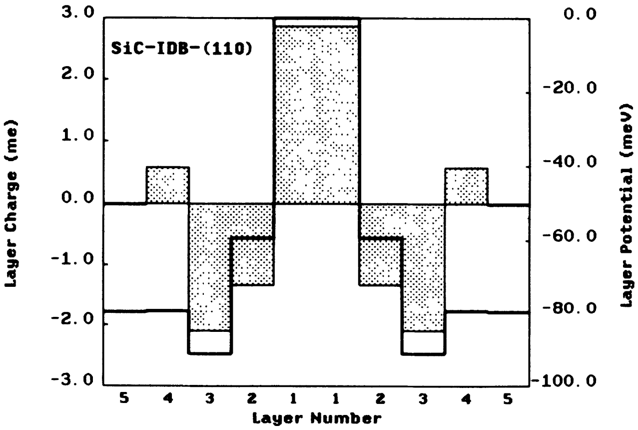

FIG. 5. Layer charge distribution and associated electrostatic potential near the unrelaxed (110) inversion domain boundary in SiC obtained from 18-layer supercell. Note: unit of charge "me" stands for 10^{-3} electron.

TABLE II. Charge distribution near IDB: the subscript refers to the layer number starting at the interface, E and E' refer to the two types of interstitial positions in bulk SiC, E has four C nearest neighbors, and E' has four Si nearest neighbors.

	Bulk	Unrelaxed	Relaxed
Si_1	1.992	2.263	2.082
C_1	4.323	4.054	4.095
E_1	0.875	0.824	0.895
E'_1	0.810	0.872	0.801
layer 1	8.000	8.013	7.873
Si_2	1.992	1.995	1.992
C_2	4.323	4.314	4.304
E_2	0.875	0.858	0.858
E'_2	0.810	0.820	0.987
layer 2	8.000	7.987	8.141
Si_3	1.992	1.994	2.000
C_3	4.323	4.324	4.285
E_3	0.875	0.871	0.859
E'_3	0.810	0.811	0.827
layer 3	8.000	8.000	7.971

the $n=9$ cell with unrelaxed geometry. An accumulation of electrons near the surface is apparent and leads to a potential difference of 80 meV between the interface and the "bulk" layers. The upwards shift of the potential near the interface is consistent with the fact that the highest valence-band states there are pushed up out of the valence band. One may notice that the potential in the $n=9$ cell used for this calculation converges to a constant bulk value and that the bulklike layer has negligible charge. This means that the cell is larger than the screening length required for establishing charge neutrality. The layer charge profiles in the smaller cells are fairly different and cannot be assumed to accurately represent that of an isolated IDB. The potential shift between bulk and interface layer is relatively small reflecting the small layer average charge density and consequently does not contribute significantly to the total energy. As pointed out above, the electrostatic contribution to the total energy is essentially related to the repulsion of the like charges near the interface.

From the charge distribution atom per atom given in Table II, we see that an electron transfer of ~ 0.2 e takes place from the C to the Si atom in the first layer. This result is obtained both in the fully self-consistent calculations for the $n=5$ superlattice and the SCDP calculations. This is consistent with the formation of a Si—Si bond at the expense of a Si—C bond. In the relaxed geometry the increase in electronic charge on the Si is reduced (consistent with an upward movement of Si—Si bonds) while the decrease in electronic charge on the C is maintained. Thus the first layer actually becomes somewhat depleted of electronic charge while the next layer away from the interface accumulates charge. As the relaxed geometry was only studied for a relatively small cell, the magnitudes of these charge redistributions may to some extent be affected by the interaction between the neighboring IDB's in the superlattice.

G. Discussion of band bending

The potential profile in the superlattice unit cell discussed above must be clearly distinguished from a band-bending effect. The latter relates to a much larger distance scale (typically a few tens to hundreds of nm). It falls outside the scope of a first-principles band-structure calculation, not only because of the macroscopic nature of the problem but also because it is a finite temperature effect. In the effort to relate the behavior in the two length scales, we encounter a long-debated question in analogous systems, metal-semiconductor contacts, and semiconductor heterojunctions. The question is whether or not localized interface states pin the Fermi level at a certain position in the gap near the interface. If that occurs, thermal equilibrium (manifested by the constancy of the Fermi level) will generally lead to a band bending.

A thorough investigation of whether or not pinning takes place would require a unified treatment of both the short-range (local electronic charge distribution near the boundary) and long-range (doping-dependent band bending) contributions to the electrostatic fields and their contribution to the total energy of the system. This would be a formidable problem for a realistic band-structure calculation. Such a unified treatment has, however, been carried out by Mailhiot and Duke[39,40] for interfaces between jellium-modeled systems. For their simplified model, they find that pinning does not occur for typical doping of the semiconductors. However, when they introduce states localized near the interface,[40] in sufficient concentration ($\geq 10^{14}$ cm^{-2}), pinning is found. These authors ascribe these localized states to atomic rearrangements, chemical reactions, or other defects near the boundary, but not to *intrinsic* states associated with a perfect interface. We believe that our intrinsic interface states, which apparently would not appear in their simplified model, would exhibit essentially the same behavior as their extrinsic states. The essential point is that both types of states alter the interface charge density. Since for our IDB there is one interface state per interface unit cell, which corresponds to about 10^{15} cm^{-2}, we believe pinning will indeed occur.

As we have discussed above, we expect this pinning of the Fermi level to occur near the bottom of the conduction band. Due to the limitations in our relaxation model and the small size of the superlattice, we cannot define the pinning position very accurately. It may either occur slightly below or slightly above the conduction-band edge, the latter corresponding to a locally (semi)metallic system. In any case, for an intrinsic semiconductor where the Fermi level in the bulk falls near the middle of the band gap, or a p-type semiconductor where the Fermi level lies near the valence-band maximum, this situation will induce a downward band bending towards the interface. The downward bending is opposite to the atomic scale potential profile of Fig. 5, which was seen to go up near the interface. This, however, is not a contradiction. The latter reflects the microscopic electronic charge distribution related to the interface states. The band bending reflects the macroscopic equilibration of the electronic chemical potential and is as such a finite temperature effect. The band bending has important consequences for the electrical transport across the IDB. In particular, the situation sketched above corresponds to a barrier for the transport of holes.

VI. CONCLUSIONS

In this work we have investigated various aspects of the electronic properties as well as the energetics of the inversion domain boundary (IDB) along the (110) crystallographic plane in SiC. The calculations used the LMTO-ASA method in the supercell geometry. The fully self-consistent LMTO approach was employed for the smallest cell studied (involving 10 layers). The more efficient restricted self-consistency version of the LMTO method that we successfully used in several previous studies was utilized for cells containing 10, 14, and 18 layers. The studies of the larger cells allowed us to more accurately obtain the electronic properties of an isolated IDB. The simplified total-energy difference expressions obtained in the frozen-potential approach were also used to analyze various contributions to the total-energy difference.

The main conclusions from the present work are as follows.

1. A high energy of formation of 5.91 eV/i.u.c.a is obtained for the unrelaxed structure of the IDB. This large energy is mainly a result of electrostatic repulsions in the Si—Si and C—C bonds at the interface. Due to the deep-lying valence levels of C, the Si and C atoms are cations and anions, respectively. It is clearly energetically unfavorable to form cation-cation or anion-anion bonds.

2. Interface localized states with considerable dispersion occur in both gaps, leading to broad features in the density of states. These remain present even after relaxation. They can qualitatively be interpreted in terms of a simple bond orbital model which shows that Si—Si bond related features are pushed up in energy and C—C bond related features are pushed down. This leads to a broadening of the various features in the density of states. The interaction with neighboring Si—C bonds produces interface states with mixed Si and C contributions. The occupied interface states cause some accumulation of electronic charge near the interface, which results in an upward potential shift near the interface, consistent with states being pushed out of the valence band. The charge mainly accumulates on Si atoms, which is consistent with the formation of Si—Si bonds.

3. Upon relaxation the highest interface band is pushed up further and enters the conduction band leading to a semimetallic system. At the same time the accumulation of charge on Si atoms near the interface is reduced. Competing trends in Si—Si and C—C bonds upon relaxation result in a net upward shift of the band-structure contribution which in turn is compensated by electrostatic contributions to the total energy. The energy is effectively lowered by 2.89 eV/i.u.c.a leading to a final energy of formation of 3.02 eV/i.u.c.a.

4. The semimetallic nature of the interface would lead to the formation of a two-dimensional electron gas near an IDB. The limited size of the superlattices investigated and uncertainties in the atomic relaxation prevent us from determining the Fermi level pinning position with sufficient accuracy to confirm the semimetallic nature of the interface with certainty. We can only confirm with certainty that the Fermi level must be pinned in the vicinity of the conduction-band minimum. This leads to a downward band bending for an intrinsic or *p*-type sample and thus has important consequences for hole transport across the IDB.

ACKNOWLEDGMENTS

We wish to thank P. Pirouz for bringing the IDB problem to our attention. This work was supported by the U.S. Defense Advanced Projects Agency–Office of Naval Research (DARPA-ONR) University Research Initiative Program at CWRU under Contract No. N000-13-86-K-0773. The computations were performed at the Pittsburgh Supercomputing Center, under Project No. PHY-87-0036P.

---

[1] See, e.g., *Amorphous and Crystalline Silicon Carbide and Related Materials,* Vol. 34 of *Proceedings in Physics,* edited by G.L. Harris and C.Y.-W. Yang (Springer, Berlin, 1989); *Novel Refractory Semiconductors,* Vol. 97 of *Materials Research Society Symposium Proceedings,* edited by D. Emin, T. Aselage, and C. Wood (MRS, Pittsburgh, 1987).

[2] S. Nishino, J. A. Powell, and H. H. Will, Appl. Phys. Lett. **42**, 460 (1983).

[3] K. Shibahara, S. Nishino, and H. Matsunami, J. Cryst. Growth. **78**, 538 (1986).

[4] J. A. Powell, L. G. Matus, M. A. Kuczmarski, C. M. Chorey, T. T. Cheng, and P. Pirouz, Appl. Phys. Lett. **51**, 823 (1987).

[5] J. D. Parsons, in *Novel Refractory Semiconductors,* Vol. 97 of *Materials Research Society Symposium Proceedings,* edited by D. Emin, T. Aselage, and C. Wood (MRS, Pittsburgh, 1987), p. 271.

[6] H. Kong, H. J. Kim, J. A. Edmond, J. W. Palmour, J. Ryu, C. H. Carter, Jr., J. T. Glass, and R. F. Davis, in Ref. 5, p. 233.

[7] R. C. Pond, in *Dislocations and Properties of Real Materials* (London Institute of Metals, London, 1987), p. 71.

[8] P. Pirouz, C. M. Chorey, and J. A. Powell, Appl. Phys. Lett. **50**, 221 (1987).

[9] D. J. Chadi, Phys. Rev. Lett. **59**, 1691 (1987).

[10] T. Nakayama, Y. Tanashiro, and K. Takayanagi, Jpn. J. Appl. Phys. Pt. 2 **26**, L280 (1987).

[11] K. Shibahara, S. Nishino, and H. Matsunani, in Ref. 5, p. 183.

[12] W. R. L. Lambrecht, B. Segall, and P. Pirouz, in *Thin Films: Stresses and Mechanical Properties,* Vol. 130 of *Materials Research Society Symposium Proceedings,* edited by J. C. Bravman, W. D. Nix, D. M. Barnett, and D. A. Smith (MRS, Pittsburgh, 1989), p. 199.

[13] T. T. Cheng, P. Pirouz, and F. Ernst, in *Advances in Materials, Processing and Devices in III-V Compound Semiconductors,* Vol. 144 of *Materials Research Society Symposium Proceedings,* edited by D. K. Sadana, L. Eastman, and R. Dupuis (MRS, Pittsburgh, 1989), p. 189.

[14] P. N. Keating, Phys. Rev. **145**, 637 (1966).

[15] R. M. Martin, Phys. Rev. B **1**, 4005 (1970).

[16] O. K. Andersen, Phys. Rev. B **12**, 3060 (1975); O. K. Andersen, O. Jepsen, and M. Šob, in *Electronic Band Structure and its Applications*, edited by M. Yussouff (Springer, Heidelberg, 1987).

[17] P. Hohenberg and W. Kohn, Phys. Rev. **136**, B864 (1964); W. Kohn and L. J. Sham, *ibid.* **140**, A1133 (1965); for a recent review, see, e.g., W. Kohn, in *Highlights of Condensed-Matter Theory,* Proceedings of the International School of Physics "Enrico Fermi," Course LXXXIX, edited by F. Bassani, F. Fumi, and M. P. Tosi (North-Holland, Amsterdam, 1985), p. 1.

[18] W. R. L. Lambrecht and B. Segall, Phys. Rev. Lett. **61**, 1764 (1988).

[19] W. R. L. Lambrecht, B. Segall, and O. K. Andersen, Phys. Rev. B **41** (to be published).

[20] W. R. L. Lambrecht and B. Segall, in *Bonding, Structure and Mechanical Properties of Metal/Ceramic Interfaces,* edited by M. Ruehle, A. G. Evans, M. F. Ashby, and J. P. Hirth (Pergamon, Oxford, 1989).

[21] W. R. L. Lambrecht and B. Segall, Phys. Rev. B **41** (to be published).

[22] J. Kollar and O. K. Andersen (unpublished results), referred to in O. K. Andersen, O. Jepsen, and D. Glötzel, in *Highlights of Condensed Matter Theory,* Proceedings of the International School of Physics "Enrico Fermi," Course LXXXIX, edited by F. Bassani, F. Fumi, and M. P. Tosi (North-Holland, Amsterdam, 1985), p. 59; a similar method without constant shifts has been used in N. E. Christensen and O. B. Christensen, Phys. Rev. B **33**, 4739 (1986).

[23] D. J. Chadi, Phys. Rev. B **29**, 785 (1984).

[24] A. P. Sutton, M. W. Finnis, D. G. Pettifor, and Y. Ohta, J. Phys. C **21**, 35 (1988).

[25] *Landolt-Börnstein Numerical Data and Functional Relationships in Science and Technology, New Series,* edited by O. Madelung (Springer, Berlin, 1982), Vol. 17a.

[26] D. D. Wagman, W. H. Evans, V. B. Parker, I. Halow, S. M. Baily, and R. H. Shumm, *Selected Values of Chemical Termodynamics Properties, Tables for the First Thirty-Four Elements in the Standard Order of Arrangement,* Natl. Bur. Stand. Tech. Note No. 270-3 (U.S. GPO, Washington, D.C., 1968).

[27] W. R. L. Lambrecht and B. Segall, Phys. Rev. B **40**, 7793 (1989).

[28] J. C. Phillips, *Bonds and Bands in Semiconductors* (Academic, New York, 1973).

[29] The Phillips *ionicity* should be compared to the square of our *polarity* because of a slightly different definition.

[30] Since we used the experimental lattice constant, which is slightly larger than our theoretical equilibrium lattice constant, a small negative pressure of -6.5 GPa is obtained for the perfect crystal.

[31] C. Cheng, R. J. Needs, and V. Heine, J. Phys. C **21**, 1049 (1988); N. Churcher, K. Kunc, and V. Heine, *ibid.* **19**, 4413 (1986).

[32] P. J. H. Denteneer and W. van Haeringen, Solid State Commun. **59**, 829 (1986); **65**, 115 (1988); Phys. Rev. B **33**, 2831 (1986).

[33] P. Pirouz, in *Polycrystalline Semiconductors,* Vol. 35 of *Springer Proceedings in Physics,* edited by J. H. Werner, H. J. Möller, and H. P. Strunk (Springer, Berlin, 1989), p. 200.

[34] C. Wang, J. Bernholc, and R. F. Davis, Phys. Rev. B **38**, 12 752 (1988).

[35] W. R. L. Lambrecht and O. K. Andersen, Surf. Sci. **178**, 256 (1986).

[36] W. A. Harrison, *Electronic Structure and Properties of Solids* (Freeman, San Francisco, 1980).

[37] W. J. Choyke, Z. C. Feng, and J. A. Powell, J. Appl. Phys. **64**, 3163 (1988).

[38] J. A. Powell, private communication.

[39] C. Mailhiot and C. B. Duke, Phys. Rev. B **33**, 1118 (1986).

[40] C. B. Duke and C. Mailhiot, J. Vac. Sci. Technol. B **3**, 1170 (1985).

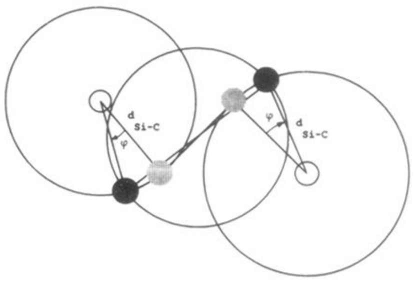

FIG. 2. Bond-rotation bond-length relaxation model. The small open circles denote C atoms, the shaded circles denote Si in the unrelaxed positions, and the solid circles denote Si in the relaxed positions. The relaxed positions are found by rotating the Si—C as indicated until the Si-Si distance of bulk diamond Si is obtained.

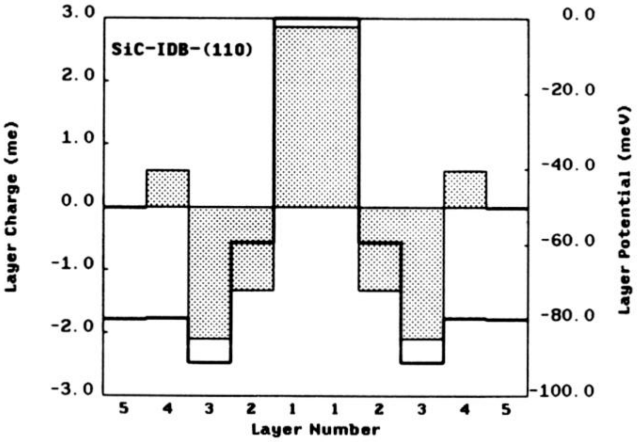

FIG. 5. Layer charge distribution and associated electrostatic potential near the unrelaxed (110) inversion domain boundary in SiC obtained from 18-layer supercell. Note: unit of charge "me" stands for 10^{-3} electron.